DALTON

Conformational polymorphism and fluxional behaviour of $M(PR_3)_2$ units in *closo*-twelve-atom metallaheteroboranes with MX_2B_9 (X = C or As) and MZB_{10} cages (Z = S, Se or Te)†

Donnacha O'Connell,[a] Jennifer C. Patterson,[a] Trevor R. Spalding,*[a] George Ferguson,*[b] John F. Gallagher,[b] Yiwei Li,[b] John D. Kennedy,*[c] Ramón Macías,[c] Mark Thornton-Pett[c] and Josef Holub[d]

[a] *Chemistry Department, University College, Cork, Ireland*
[b] *Chemistry Department, University of Guelph, Guelph, Ontario, N1G 2W1, Canada*
[c] *School of Chemistry, University of Leeds, Leeds LS2 9JT, UK*
[d] *Institute of Inorganic Chemistry, Academy of Sciences of the Czech Republic, 25068 Řež near Prague, The Czech Republic*

The compounds [3,3-$(PEt_3)_2$-*closo*-3,1,2-$PtAs_2B_9H_9$] **1** and [2,2-$(PMe_2Ph)_2$-*closo*-2,1-$PtSB_{10}H_{10}$] **2** were synthesised and characterised by NMR spectroscopy and X-ray crystallography. Crystals of **1** exhibit conformational polymorphism with five conformers of the $Pt(PEt_3)_2$ unit above the As_2B_3 face; those of **2** contain single conformers. The free energy of the barrier to rotation of the $Pt(PMe_2Ph)_2$ unit above the SB_{10} cage ligand in **2** has been determined in chloroform solution and is compared with data from other platinum and palladium metallaheteroboranes containing $C_2B_9H_{11}$, $As_2B_9H_9$, $SeB_{10}H_{10}$ and $TeB_{10}H_{10}$ ligands. A mechanism for the rotation of $M(PR_3)_2$ units above heteroborane ligand faces is suggested. It involves shifting the $M(PR_3)_2$ unit *via* η^n-bonded species ($n < 5$) with a concomitant twisting of the $M(PR_3)_2$ unit about an axis passing approximately through the metal atom and the antipodal B atom.

For a series of platinaheteroboranes with *closo*-type twelve-vertex cluster structures, effective rotational fluxionalities of $Pt(PMe_2Ph)_2$ units above the five-atom faces of the ligands $C_2B_9H_{11}$[2] and $As_2B_9H_9$[3] **Ia**, and $SeB_{10}H_{10}$[4] and $TeB_{10}H_{10}$[5] **Ib** have been reported to occur in solution, and the free-energy barriers to rotation, $\Delta G^{\ddagger}$, have been measured. Likewise, equivalent data have been reported for palladium units $Pd(PMe_2Ph)_2$ and $PdCl(PMe_2Ph)$ rotating above $As_2B_9H_9$ ligands.[3] The reported values of $\Delta G^{\ddagger}$ vary from 62 to less than 30 kJ mol^{-1}. In all cases the metal–phosphine unit appears to rotate about an axis which passes approximately through the metal atom and the antipodal B atom. Previously, molecular orbital studies of metal–ligand interactions in metallacarbaboranes using the $Pt(PH_3)_2$ unit as a model have been interpreted to show that there are distinct general preferences for the conformation of $Pt(PR_3)_2$ units above the ligand.[6] Diagrams **IIa** and **IIb** show the proposed preferred conformations of metal units above C_2B_3 faces, and **IIc** shows that above a CB_4 face.[6] Generally, single conformers have been hitherto observed in the crystal structures of twelve-vertex platina- and palladadicarbaboranes,[6-9] and platinaselena-[4] and platinatelluraboranes[5] (**IIc** where X = Se or Te). However, this is not always the case. For example, crystals of [3,3-$(PMe_2Ph)_2$-*closo*-3,1,2-$PtC_2B_9H_{11}$] **3**[2] and [3,3-$(PPh_3)_2$-*closo*-3,1,2-$PtAs_2B_9H_9$] **4**[3] contain mixtures of rotational conformers, *i.e.* they exhibit conformational polymorphism within a single crystal. Similar effects have recently been reported in organometallic chemistry, most notably in a study of the [1,2-bis(diethylphosphino)-ethane]nickel complex of anthracene[10] and also, but perhaps less strikingly, in a study of the metal cluster compound $[Ru_6C(CO)_{17}]$.[11]

We now report a further example of conformational polymorphism in twelve-vertex *closo*-metallaheteroborane chemistry which is observed in the compound [3,3-$(PEt_3)_2$-*closo*-3,1,2-$PtAs_2B_9H_9$] **1**. We also make the general observation that compounds with a low free-energy barrier to rotation ($\Delta G^{\ddagger}$ of the same order as that of crystal-packing forces) may crystallise as a mixture of conformational

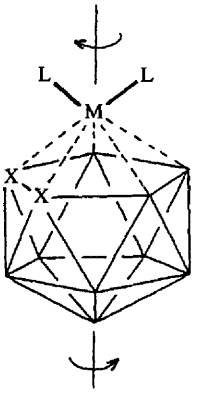

Ia X = C or As

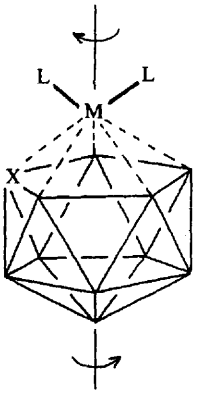

Ib X = Se or Te

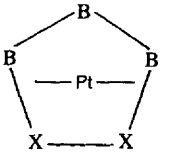

IIa X = C or As

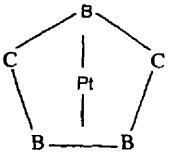

IIb

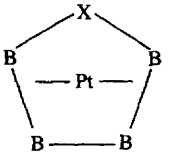

IIc X = C, Se or Te

† Metallaheteroborane chemistry. Part 13.[1]

polymorphs. Additionally, our data indicate that compounds with higher $\Delta G^{\ddagger}$ values for complete rotation such as [2,2-$(PMe_2Ph)_2$-*closo*-2,1-$PtXB_{10}H_{10}$] (X = S **2**, Se or Te) or [2,2-$(PMe_2Ph)_2$-*closo*-2,1,8-$PtC_2B_9H_{11}$] **5** could also in principle exhibit different solid-state conformers although no examples have been reported as yet. Finally, a general mechanism is suggested to take account of the presently known features of the rotational processes observed in solution for **1**, **2**, **5** and related compounds. Aspects of this mechanism are discussed with reference to observations both from solution studies and from crystallographic studies of some organometallic[10,11] compounds and of some rhodacarbaborane compounds with the general formulation [$\{Rh(PR_3)_2H\}C_2B_9H_{11}$].[12,13] The results and conclusions in this paper also suggest that a supposition[8] concerning the origin of the cage distortion and conformer 'twisting' in the structure of the previously reported platinadicarbaborane [1-Ph-3,3-$(PMe_2Ph)_2$-*closo*-3,1,2-$PtC_2B_9H_{10}$] **6** may be wrong.

Results and Discussion

Syntheses of [3,3-$(PEt_3)_2$-*closo*-3,1,2-$PtAs_2B_9H_9$] 1, [2,2-$(PMe_2Ph)_2$-*closo*-2,1-$PtSB_{10}H_{10}$] 2, [3,3-$(PMe_2Ph)_2$-*closo*-3,1,2-$PtC_2B_9H_{11}$] 3 and [2,2-$(PMe_2Ph)_2$-*closo*-2,1,8-$PtC_2B_9H_{11}$] 5

Compound **1** was synthesised from a mixture of equimolar amounts of [NMe_4][*nido*-7,8-$As_2B_9H_{10}$] and *cis*-[$PtCl_2(PEt_3)_2$] with an excess of triethylamine in ethanol. The mixture was subjected to microwave irradiation for 8 min. The reaction afforded the red compound [3,3-$(PEt_3)_2$-*closo*-3,1,2-$PtAs_2B_9H_9$] **1** in 65% yield. Compound **2**, [2,2-$(PMe_2Ph)_2$-*closo*-2,1-$PtSB_{10}H_{10}$], was obtained as a pale yellow solid in 11% yield from the reaction between *cis*-[$PtCl_2(PMe_2Ph)_2$], *nido*-7-$SB_{10}H_{12}$ and *N,N,N',N'*-tetramethylnaphthalene-1,8-diamine, *i.e.* 'proton sponge', in CH_2Cl_2 solution at room temperature for 8 h.

Two procedures were used to synthesise compounds **3** and **5**. In the first, equimolar amounts of Cs[*nido*-7,8-$C_2B_9H_{12}$] and *cis*-[$PtCl_2(PMe_2Ph)_2$] in ethanol in the presence of a ten-fold excess of triethylamine were irradiated with microwave radiation for 30 min.[8,14] The reaction pressure was not allowed to exceed 10 atm (*ca.* 10^6 Pa) and the maximum reaction temperature was 100 °C. The pale orange compound **3** and the yellow compound **5** were isolated in yields of 4% and 19% respectively. In an alternative procedure[2] the same amounts of reactants in ethanol solvent were heated at reflux at atmospheric pressure for 6 d and afforded **3** and **5** in yields of 26 and 4% respectively. In a separate experiment a sample of [3,3-$(PMe_2Ph)_2$-*closo*-3,1,2-$PtC_2B_9H_{11}$] **3** in ethanol was subjected to microwave irradiation for 10 min and [2,2-$(PMe_2Ph)_2$-*closo*-2,1,8-$PtC_2B_9H_{11}$] **5** was isolated in 90% yield. When an ethanolic solution of the caesium salt of the [*nido*-7,8-$C_2B_9H_{12}$]$^-$ anion with an excess of triethylamine was subjected to microwave irradiation for 30 min no rearrangement occurred. It is clear from these experiments that **3** rearranged to **5** and, since the [*nido*-7,8-$C_2B_9H_{12}$]$^-$ anion itself did not rearrange, **5** was not formed from a reaction between *cis*-[$PtCl_2(PMe_2Ph)_2$] and an isomer of the [*nido*-7,8-$C_2B_9H_{12}$]$^-$ anion.

Salient features in the IR spectra of compounds **1**–**3** and **5** were due to the strong absorptions of terminal B–H bonds in the region 2600–2400 cm^{-1}.

X-Ray analyses of compounds 1 and 2

X-Ray diffraction analyses confirmed that the platinadiarsaborane **1** and the platinathiaborane **2** contain *closo*-type twelve-atom cluster skeletons (Figs. 1 and 2). Selected interatomic distances and angles are given in Tables 1 and 2 respectively. The ranges of Pt–P and B–B distances in **1** are similar

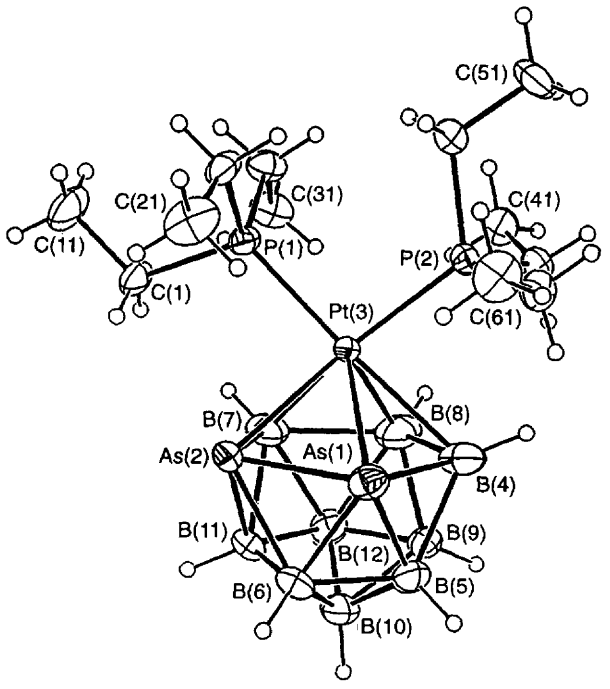

Fig. 1 View of the compound [3,3-$(PEt_3)_2$-*closo*-3,1,2-$PtAs_2B_9H_9$] **1** showing the numbering scheme

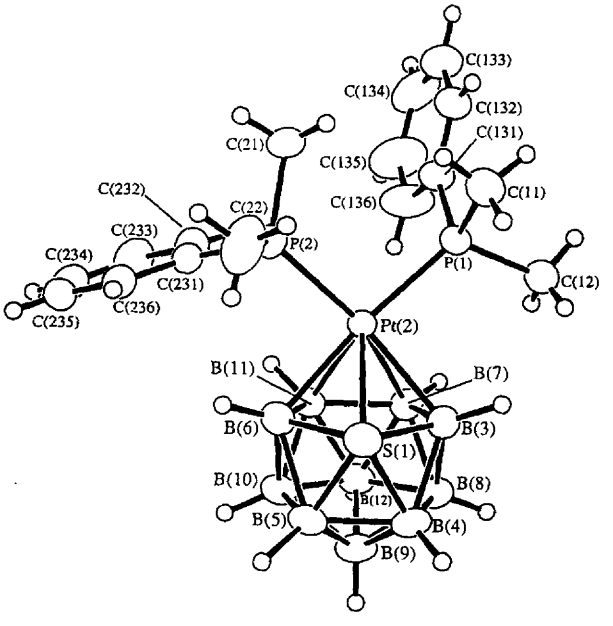

Fig. 2 View of the compound [2,2-$(PMe_2Ph)_2$-*closo*-2,1-$PtSB_{10}H_{10}$] **2** showing the numbering scheme

to those in other platinadiarsenaboranes,[3,15] and there is a general resemblance between the corresponding distances in **2** and the equivalent selenium and tellurium compounds,[4,5] apart of course from the lengthening of the distances to the Se or Te atoms compared to the S atom in **2**.

A remarkable feature is observed in the crystal structure of the $\{PtAs_2B_9\}$ species **1**, which in some respects may be considered to be an extension of the situation previously found in the $\{PtC_2B_9\}$ species **3** where two conformers existed in the asymmetric unit.[2] In **1** significant occupancy by arsenic atoms is observed in all five positions in the As_2B_3 face bonded to platinum. The disorder affects the refined values of the associated As–B and B–B distances, Table 1, and a detailed discussion of these distances is thus curtailed. The values are effectively the averages for the five conformers present in the crystal and should not be taken as the distances in any

Table 1 Selected interatomic distances (Å) and angles (°) for [3,3-$(PEt_3)_2$-*closo*-3,1,2-$PtAs_2B_9H_9$] **1** with estimated standard deviations (e.s.d.s) in parentheses

As(1)–As(2)	2.4594(15)	B(4)–B(9)	1.934(9)	As(2)–B(11)	2.097(10)	B(7)–B(12)	1.910(9)
As(1)–Pt(3)	2.6656(11)	B(5)–B(6)	1.802(14)	Pt(3)–B(4)	2.471(4)	B(8)–B(9)	1.903(11)
As(1)–B(4)	2.320(4)	B(5)–B(9)	1.787(14)	Pt(3)–B(7)	2.489(4)	B(8)–B(12)	1.904(11)
As(1)–B(5)	2.098(9)	B(5)–B(10)	1.757(15)	Pt(3)–B(8)	2.508(6)	B(9)–B(10)	1.757(13)
As(1)–B(6)	2.175(11)	B(6)–B(10)	1.761(15)	Pt(3)–P(1)	2.3183(18)	B(9)–B(12)	1.751(14)
As(2)–Pt(3)	2.5412(10)	B(6)–B(11)	1.847(16)	Pt(3)–P(2)	2.3235(16)	B(10)–B(11)	1.776(14)
As(2)–B(6)	2.174(11)	B(7)–B(8)	2.151(7)	B(4)–B(5)	1.993(10)	B(10)–B(12)	1.769(15)
As(2)–B(7)	2.405(4)	B(7)–B(11)	1.974(11)	B(4)–B(8)	2.196(7)	B(11)–B(12)	1.772(14)
As(2)–As(1)–Pt(3)	59.29(4)	B(10)–B(6)–B(11)	58.9(6)	P(1)–Pt(3)–P(2)	96.93(6)	B(10)–B(9)–B(12)	60.6(6)
As(2)–As(1)–B(4)	100.98(11)	As(2)–B(7)–Pt(3)	62.53(11)	As(1)–B(4)–Pt(3)	67.53(10)	B(5)–B(10)–B(6)	61.6(6)
As(2)–As(1)–B(6)	55.5(3)	As(2)–B(7)–B(8)	109.9(3)	As(1)–B(4)–B(5)	57.6(3)	B(5)–B(10)–B(9)	61.1(6)
Pt(3)–As(1)–B(4)	58.95(9)	As(2)–B(7)–B(11)	56.2(3)	As(1)–B(4)–B(8)	114.8(3)	B(6)–B(10)–B(11)	62.9(6)
B(4)–As(1)–B(5)	53.4(3)	Pt(3)–B(7)–B(8)	64.95(18)	Pt(3)–B(4)–B(8)	64.68(17)	B(9)–B(10)–B(12)	59.6(6)
B(5)–As(1)–B(6)	49.9(4)	B(8)–B(7)–B(12)	55.5(3)	B(5)–B(4)–B(9)	54.1(4)	B(11)–B(10)–B(12)	60.0(6)
As(1)–As(2)–Pt(3)	64.40(3)	B(11)–B(7)–B(12)	54.2(4)	B(8)–B(4)–B(9)	54.4(3)	As(2)–B(11)–B(6)	66.5(5)
As(1)–As(2)–B(6)	55.6(3)	Pt(3)–B(8)–B(4)	62.97(17)	As(1)–B(5)–B(4)	69.0(3)	As(2)–B(11)–B(7)	72.4(3)
As(1)–As(2)–B(7)	105.36(11)	Pt(3)–B(8)–B(7)	64.05(19)	As(1)–B(5)–B(6)	67.3(5)	B(6)–B(11)–B(10)	58.1(6)
Pt(3)–As(2)–B(7)	60.35(10)	B(4)–B(8)–B(7)	109.0(3)	B(4)–B(5)–B(9)	61.3(4)	B(7)–B(11)–B(12)	61.0(5)
B(6)–As(2)–B(11)	51.2(4)	B(4)–B(8)–B(9)	55.7(3)	B(6)–B(5)–B(10)	59.3(6)	B(10)–B(11)–B(12)	59.8(6)
B(7)–As(2)–B(11)	51.5(3)	B(7)–B(8)–B(12)	55.8(3)	B(9)–B(5)–B(10)	59.4(5)	B(7)–B(12)–B(8)	68.7(4)
As(1)–Pt(3)–As(2)	56.31(4)	B(9)–B(8)–B(12)	54.8(4)	As(1)–B(6)–As(2)	68.9(3)	B(7)–B(12)–B(11)	64.7(4)
As(1)–Pt(3)–B(4)	53.53(9)	B(4)–B(9)–B(5)	64.6(4)	As(1)–B(6)–B(5)	62.9(4)	B(8)–B(12)–B(9)	62.6(5)
As(2)–Pt(3)–B(7)	57.12(10)	B(4)–B(9)–B(8)	69.8(3)	As(2)–B(6)–B(11)	62.3(4)	B(9)–B(12)–B(10)	59.9(6)
B(4)–Pt(3)–B(8)	52.35(14)	B(5)–B(9)–B(10)	59.4(6)	B(5)–B(6)–B(10)	59.1(6)	B(10)–B(12)–B(11)	60.2(6)
B(7)–Pt(3)–B(8)	51.00(15)	B(8)–B(9)–B(12)	62.6(5)				

Table 2 Selected interatomic distances (Å) and angles (°) for [2,2-$(PMe_2Ph)_2$-*closo*-2,1-$PtSB_{10}H_{10}$] **2** with e.s.d.s in parentheses

Pt(2)–P(1)	2.2870(7)	Pt(2)–P(2)	2.3021(7)	B(4)–B(5)	1.840(5)	B(7)–B(11)	1.821(4)
Pt(2)–S(1)	2.6633(7)			B(4)–B(8)	1.761(5)	B(5)–B(10)	1.777(5)
Pt(2)–B(3)	2.318(3)	Pt(2)–B(6)	2.296(3)	B(4)–B(9)	1.757(5)	B(5)–B(9)	1.750(5)
Pt(2)–B(7)	2.230(3)	Pt(2)–B(11)	2.248(3)	B(7)–B(8)	1.790(4)	B(10)–B(11)	1.776(5)
S(1)–B(3)	2.034(3)	S(1)–B(6)	2.060(3)	B(7)–B(12)	1.768(5)	B(11)–B(12)	1.771(4)
S(1)–B(4)	1.979(3)	S(1)–B(5)	1.973(4)	B(8)–B(9)	1.800(5)	B(9)–B(10)	1.785(5)
B(3)–B(4)	1.919(5)	B(5)–B(6)	1.938(5)	B(8)–B(12)	1.789(5)	B(10)–B(12)	1.778(5)
B(3)–B(7)	1.848(4)	B(6)–B(11)	1.836(4)	B(9)–B(12)	1.769(5)		
B(3)–B(8)	1.781(4)	B(6)–B(10)	1.785(4)				
B(7)–Pt(2)–B(11)	47.99(11)	B(7)–Pt(2)–B(3)	47.90(11)	B(10)–B(6)–B(5)	56.8(2)	B(11)–B(7)–B(3)	108.7(2)
B(11)–Pt(2)–B(6)	47.66(11)	B(6)–Pt(2)–S(1)	48.39(8)	B(12)–B(7)–B(8)	60.4(2)	B(3)–B(7)–Pt(2)	68.55(14)
P(1)–Pt(2)–P(2)	95.46(3)	B(3)–Pt(2)–S(1)	47.58(8)	B(8)–B(7)–B(3)	58.6(2)	B(4)–B(8)–B(3)	65.6(2)
B(5)–S(1)–B(4)	55.5(2)	B(5)–S(1)–B(6)	57.39(13)	B(11)–B(7)–Pt(2)	66.51(13)	B(12)–B(8)–B(7)	59.2(2)
B(4)–S(1)–B(3)	57.11(14)	B(3)–S(1)–B(6)	92.39(13)	B(3)–B(8)–B(7)	62.4(2)	B(5)–B(9)–B(4)	63.3(2)
B(3)–S(1)–Pt(2)	57.28(9)	B(6)–S(1)–Pt(2)	56.44(9)	B(4)–B(8)–B(9)	59.1(2)	B(12)–B(9)–B(8)	60.2(2)
B(8)–B(3)–B(7)	59.1(2)	B(4)–B(3)–S(1)	59.99(14)	B(12)–B(8)–B(9)	59.1(2)	B(12)–B(10)–B(9)	59.5(2)
B(7)–B(3)–S(1)	115.5(2)	B(7)–B(3)–Pt(2)	63.55(13)	B(5)–B(9)–B(10)	60.3(2)	B(5)–B(10)–B(6)	65.9(2)
B(8)–B(3)–B(4)	56.7(2)	S(1)–B(3)–Pt(2)	75.14(10)	B(12)–B(9)–B(10)	60.0(2)	B(7)–B(11)–B(6)	107.1(2)
B(9)–B(4)–B(8)	61.5(2)	B(3)–B(4)–S(1)	62.90(14)	B(4)–B(9)–B(8)	59.3(2)	B(6)–B(11)–Pt(2)	67.54(13)
B(8)–B(4)–B(3)	57.7(2)	B(9)–B(4)–B(5)	58.2(2)	B(11)–B(10)–B(12)	59.8(2)	B(12)–B(11)–B(7)	58.9(2)
B(5)–B(4)–S(1)	62.1(2)	B(9)–B(5)–B(4)	58.6(2)	B(11)–B(10)–B(6)	62.1(2)	B(7)–B(12)–B(11)	61.9(2)
B(9)–B(5)–B(10)	60.8(2)	B(6)–B(5)–S(1)	63.56(14)	B(5)–B(10)–B(9)	58.9(2)	B(9)–B(12)–B(10)	60.4(2)
B(10)–B(5)–B(6)	57.2(2)	B(5)–B(6)–S(1)	59.05(13)	B(10)–B(11)–B(6)	59.2(2)	B(7)–B(12)–B(8)	60.4(2)
B(4)–B(5)–S(1)	62.4(2)	B(11)–B(6)–Pt(2)	64.79(13)	B(7)–B(11)–Pt(2)	65.50(13)	B(11)–B(12)–B(10)	60.1(2)
B(10)–B(6)–B(11)	58.7(2)	S(1)–B(6)–Pt(2)	75.17(10)	B(12)–B(11)–B(10)	60.2(2)	B(9)–B(12)–B(8)	60.8(2)
B(11)–B(6)–S(1)	116.1(2)	B(12)–B(7)–B(11)	59.1(2)				

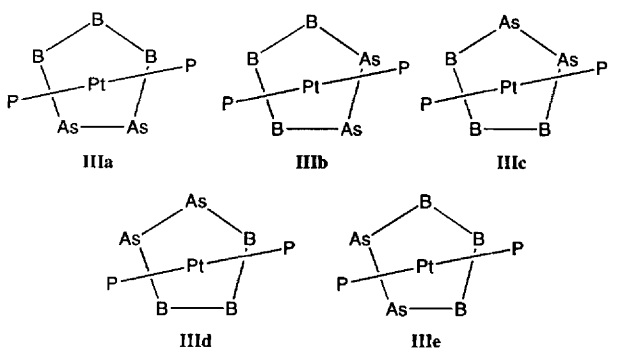

particular conformer. Thus, all five conformers shown in **IIIa**–**IIIe** are effectively observed in the crystal structure of **1** and hence all platinum–cage distances in Table 1 are actually Pt–(As/B) distances. The energy difference between **IIIb** and **IIIe**, and **IIIc** and **IIId**, will be small. Using the occupancy factors determined in the structure refinement, and assuming that all the conformers have arsenic atoms in adjacent positions, the following percentages were calculated for the conformers: **a**, 53; **b**, 12; **c**, 9; **d**, 11; **e**, 15%. This suggests that successive steps in the rotation of the $Pt(PEt_3)_2$ entity above the As_2B_3 face in **1** require very little energy. Put another way, in crystals of **1** the molecular packing is determined by the orientation of the $(Et_3P)_2Pt$ unit relative to the $As_2B_9H_9$ ligand

and adjacent molecules and the precise orientation of the $As_2B_9H_9$ cage is relatively less important. Hence, in **1** it would appear that an arsenic atom is not too dissimilar from a BH unit in effective bulk and that there is little difference in packing energetics among the conformers present. Here it is relevant that (*a*) there were two conformers present in crystals of [3,3-$(PPh_3)_2$-*closo*-3,1,2-$PtAs_2B_9H_9$] **4** and (*b*) in [3,3-$(PMe_2Ph)_2$-*closo*-3,1,2-$PtAs_2B_9H_9$] **7** the free-energy of the barrier to complete rotation of the $As_2B_9H_9$ ligand relative to the $Pt(PMe_2Ph)_2$ unit has been estimated to be less than 30 kJ mol^{-1}.[3]

Preliminary descriptions of the platinadicarbaboranes **3** and **5** have been reported[2] and their structures are shown in Figs. 3 and 4. The solid-state structure of the $\{Pt(PMe_2Ph)_2\}$ compound **3** is remarkable in that two different rotational conformers are present separately in the crystallographic asymmetric unit as distinct from the conformer disorder observed in the metalladiarsaboranes **1** and **4**. The Pt–P, B–B and B–C distances in the platinadicarbaboranes **3** and **5**, Tables 3 and 4 respectively, are comparable to literature data for related compounds.[6–9] In [3,3-$(PMe_2Ph)_2$-*closo*-3,1,2-$PtC_2B_9H_{11}$] **3** the cage C and B sites were readily distinguishable in the two structural isomers, and Pt–B and Pt–C distances were obtained (Table 3). These isomers, **3A** and **3B**, clearly have different platinum-to-cage bonding as well as different conformations of the PtP_2 unit relative to the C_2B_9 ligand [Fig. 3(*a*) and 3(*b*)].[2] Based on the Pt–B and Pt–C distances, it was suggested in the preliminary note that the Pt-to-C_2B_3 cage bonding in **3A** is essentially η^4 to a CB_3 set of atoms with a weaker fifth interaction to C(1), whereas the bonding in **3B** is more typical of a 'slipped' η^5 bonding mode between the metal atom and the C_2B_3 face.[6] Alternatively, the bonding in **3B** could be described as essentially η^3 to the three boron atoms in the face of the $C_2B_9H_{11}$ ligand with much weaker fourth and fifth interactions to C(1) and C(2). With respect to these distinct differences in hapticity of metal–ligand bonding in the two conformers of **3**, it is notable that co-ordination isomerism within a single crystal is an extremely rare phenomenon since the species concerned must be almost isoenergetic. Until recently, all previously known cases involved ionic compounds. The first example of a non-ionic compound was an organo-metallic reported in 1993,[10] *i.e.* the anthracene complex of Ni(depe) [depe = 1,2-bis(diethylphosphino)-ethane] which was observed to crystallise with two nickel environments. One contained the expected η^4-bonded Ni atom but the other had η^3-bonded nickel. The Ni–C(1) distance in the η^4-bonded complex was 2.176(8) Å compared with the equivalent (non-bonded) distance of 2.824(8) Å in the η^3-bonded molecule.[10]

Two other features are noteworthy with respect to the bonding between the PtP_2 unit and the C_2B_3 faces in the two molecules of [3,3-$(PMe_2Ph)_2$-*closo*-3,1,2-$PtC_2B_9H_{11}$] **3**. First, the difference between the two Pt–P distances in **3A** is much greater than in **3B**, *i.e.* 0.0522 compared to 0.0106 Å. In both molecules the Pt–P vector which is transoid to a PtCB triangular face of the cage is longer than the Pt–P vector transoid to a PtB_2 face. Secondly, in **3B** the C–C distance of 1.496(10) Å is shorter than a typical sp^3–sp^3 C–C distance of 1.54 Å, whereas in **3A** it is longer at 1.571(11) Å. Presumably, some electron density has been diverted from C–C into Pt–C bonding in **3A**. Finally, with respect to the discussion of the structure of **3**, a comment on a suggestion in a recent paper co-authored by some of us (D. O.'C. and T. R. S.) is in order.[8] The suggestion was that the steric influence of the phenyl substituent on the

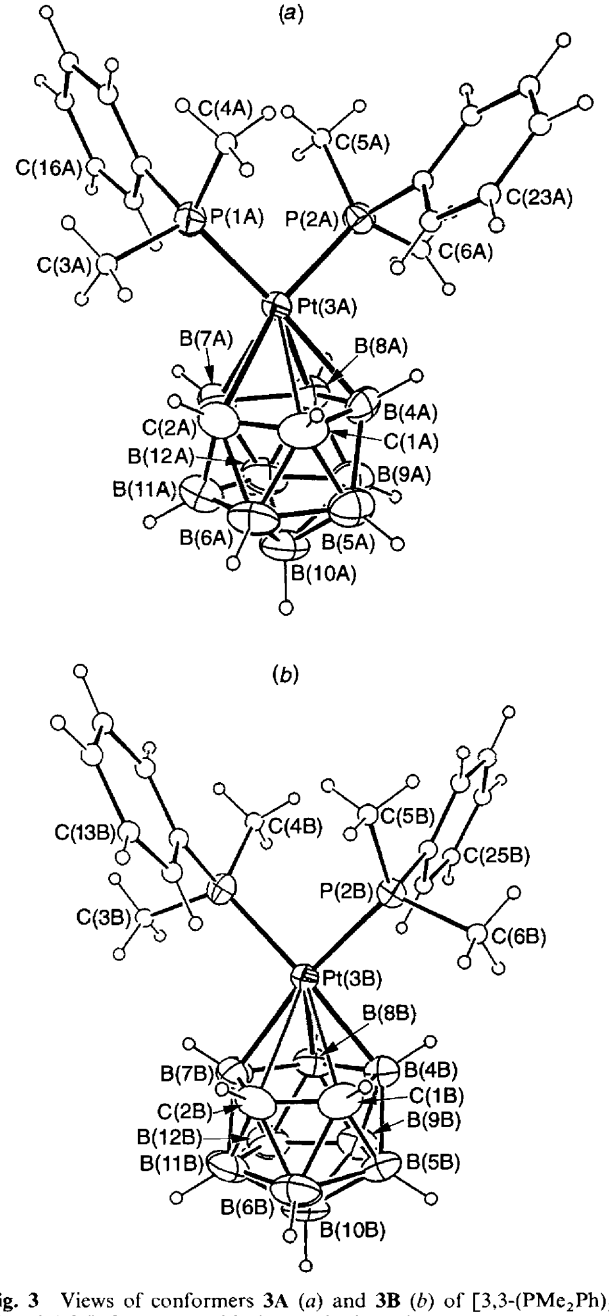

Fig. 3 Views of conformers **3A** (*a*) and **3B** (*b*) of [3,3-$(PMe_2Ph)_2$-*closo*-3,1,2-$PtC_2B_9H_{11}$] with the numbering schemes

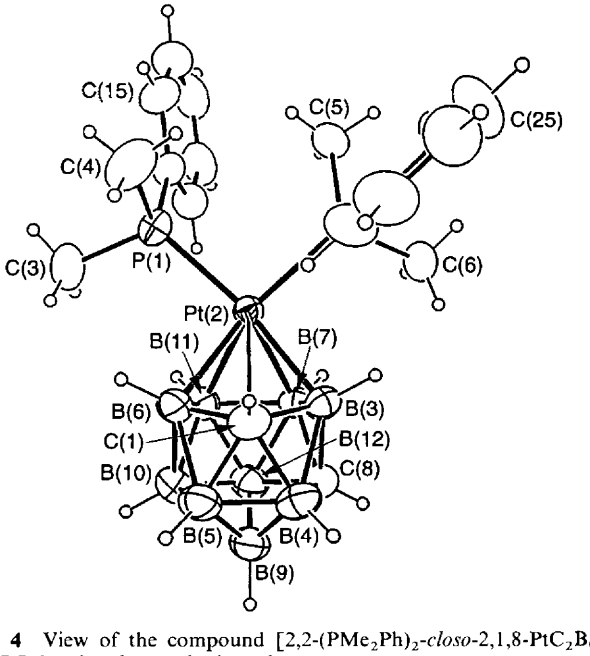

Fig. 4 View of the compound [2,2-$(PMe_2Ph)_2$-*closo*-2,1,8-$PtC_2B_9H_{11}$] **5** showing the numbering scheme

Table 3 Selected interatomic distances (Å) and angles (°) for both conformers **3A** and **3B** of [3,3-$(PMe_2Ph)_2$-*closo*-3,1,2-$PtC_2B_9H_{11}$] **3** with e.s.d.s in parentheses

Pt(3A)–P(1A)	2.2875(16)	Pt(3B)–P(1B)	2.2599(16)	B(4A)–B(9A)	1.765(11)	B(4B)–B(9B)	1.785(10)
Pt(3A)–P(2A)	2.2353(16)	Pt(3B)–P(2B)	2.2705(15)	B(5A)–B(6A)	1.733(14)	B(5B)–B(6B)	1.773(13)
Pt(3A)–C(1A)	2.515(6)	Pt(3B)–C(1B)	2.529(6)	B(5A)–B(9A)	1.752(12)	B(5B)–B(9B)	1.768(11)
Pt(3A)–C(2A)	2.302(7)	Pt(3B)–C(2B)	2.574(6)	B(5A)–B(10A)	1.758(12)	B(5B)–B(10B)	1.790(11)
Pt(3A)–B(4A)	2.307(7)	Pt(3B)–B(4B)	2.264(7)	B(6A)–B(10A)	1.747(13)	B(6B)–B(10B)	1.729(13)
Pt(3A)–B(8A)	2.265(7)	Pt(3B)–B(8B)	2.260(7)	B(6A)–B(11A)	1.795(15)	B(6B)–B(11B)	1.716(14)
Pt(3A)–B(7A)	2.284(8)	Pt(3B)–B(7B)	2.266(7)	B(8A)–B(9A)	1.762(12)	B(8B)–B(9B)	1.767(11)
C(1A)–C(2A)	1.571(11)	C(1B)–C(2B)	1.496(10)	B(8A)–B(7A)	1.789(11)	B(8B)–B(7B)	1.804(12)
C(1A)–B(4A)	1.667(9)	C(1B)–B(4B)	1.748(10)	B(8A)–B(12A)	1.758(11)	B(8B)–B(12B)	1.747(11)
C(1A)–B(5A)	1.683(11)	C(1B)–B(5B)	1.662(10)	B(9A)–B(10A)	1.805(12)	B(9B)–B(10B)	1.769(12)
C(1A)–B(6A)	1.687(11)	C(1B)–B(6B)	1.728(11)	B(9A)–B(12A)	1.755(13)	B(9B)–B(12B)	1.753(13)
C(2A)–B(6A)	1.781(11)	C(2B)–B(6B)	1.688(11)	B(10A)–B(11A)	1.750(14)	B(10B)–B(11B)	1.748(14)
C(2A)–B(11A)	1.731(12)	C(2B)–B(11B)	1.637(11)	B(10A)–B(12A)	1.742(13)	B(10B)–B(12B)	1.756(11)
C(2A)–B(7A)	1.737(12)	C(2B)–B(7B)	1.712(10)	B(11A)–B(7A)	1.738(12)	B(11B)–B(7B)	1.781(12)
B(4A)–B(5A)	1.826(11)	B(4B)–B(5B)	1.795(10)	B(11A)–B(12A)	1.737(15)	B(11B)–B(12B)	1.793(15)
B(4A)–B(8A)	1.826(10)	B(4B)–B(8B)	1.783(10)	B(7A)–B(12A)	1.753(13)	B(7B)–B(12B)	1.809(12)
P(1A)–Pt(3A)–P(2A)	93.11(6)	P(1B)–Pt(3B)–P(2B)	92.33(6)	B(10A)–B(6A)–B(11A)	59.2(5)	B(10B)–B(6B)–B(11B)	61.0(6)
C(1A)–Pt(3A)–C(2A)	37.7(3)	C(1B)–Pt(3B)–C(2B)	34.09(22)	Pt(3A)–B(8A)–B(4A)	67.7(3)	Pt(3B)–B(8B)–B(4B)	66.9(3)
C(1A)–Pt(3A)–B(4A)	40.16(23)	C(1B)–Pt(3B)–B(4B)	42.33(24)	Pt(3A)–B(8A)–B(7A)	67.4(4)	Pt(3B)–B(8B)–B(7B)	66.7(3)
C(2A)–Pt(3A)–B(7A)	44.5(3)	C(2B)–Pt(3B)–B(7B)	40.8(3)	B(4A)–B(8A)–B(9A)	58.9(4)	B(4B)–B(8B)–B(9B)	60.4(4)
B(4A)–Pt(3A)–B(8A)	47.1(3)	B(4B)–Pt(3B)–B(8B)	46.4(3)	B(4A)–B(8A)–B(7A)	104.0(5)	B(4B)–B(8B)–B(7B)	100.7(5)
B(8A)–Pt(3A)–B(7A)	46.3(3)	B(8B)–Pt(3B)–B(7B)	47.0(3)	B(9A)–B(8A)–B(12A)	59.8(5)	B(9B)–B(8B)–B(12B)	59.8(5)
Pt(3A)–C(1A)–C(2A)	63.8(3)	Pt(3B)–C(1B)–C(2B)	74.6(3)	B(7A)–B(8A)–B(12A)	59.2(5)	B(7B)–B(8B)–B(12B)	61.2(5)
Pt(3A)–C(1A)–B(4A)	63.2(3)	Pt(3B)–C(1B)–B(4B)	60.7(3)	B(4A)–B(9A)–B(5A)	62.6(4)	B(4B)–B(9B)–B(5B)	60.7(4)
C(2A)–C(1A)–B(4A)	106.9(5)	C(2B)–C(1B)–B(4B)	112.7(5)	B(4A)–B(9A)–B(8A)	62.4(4)	B(4B)–B(9B)–B(8B)	60.2(4)
C(2A)–C(1A)–B(6A)	66.2(5)	C(2B)–C(1B)–B(6B)	62.7(5)	B(5A)–B(9A)–B(10A)	59.2(5)	B(5B)–B(9B)–B(10B)	60.8(5)
B(4A)–C(1A)–B(5A)	66.0(5)	B(4B)–C(1B)–B(5B)	63.5(4)	B(8A)–B(9A)–B(12A)	60.0(5)	B(8B)–B(9B)–B(12B)	59.5(5)
B(5A)–C(1A)–B(6A)	61.9(5)	B(5B)–C(1B)–B(6B)	63.0(5)	B(10A)–B(9A)–B(12A)	58.6(5)	B(10B)–B(9B)–B(12B)	59.8(5)
Pt(3A)–C(2A)–C(1A)	78.5(4)	Pt(3B)–C(2B)–C(1B)	71.3(3)	B(5A)–B(10A)–B(6A)	59.2(5)	B(5B)–B(10B)–B(6B)	60.5(5)
Pt(3A)–C(2A)–B(7A)	67.2(3)	Pt(3B)–C(2B)–B(7B)	59.9(3)	B(5A)–B(10A)–B(9A)	58.9(5)	B(5B)–B(10B)–B(9B)	59.6(4)
C(1A)–C(2A)–B(6A)	60.1(5)	C(1B)–C(2B)–B(6B)	65.4(5)	B(6A)–B(10A)–B(11A)	61.8(6)	B(6B)–B(10B)–B(11B)	59.1(6)
C(1A)–C(2A)–B(7A)	116.8(5)	C(1B)–C(2B)–B(7B)	110.2(5)	B(9A)–B(10A)–B(12A)	59.3(5)	B(9B)–B(10B)–B(12B)	59.7(5)
B(6A)–C(2A)–B(11A)	61.5(5)	B(6B)–C(2B)–B(11B)	62.1(5)	B(11A)–B(10A)–B(12A)	59.7(6)	B(11B)–B(10B)–B(12B)	61.6(6)
B(11A)–C(2A)–B(7A)	60.2(5)	B(11B)–C(2B)–B(7B)	64.2(5)	C(2A)–B(11A)–B(6A)	60.6(5)	C(2B)–B(11B)–B(6B)	60.4(5)
Pt(3A)–B(4A)–C(1A)	76.7(3)	Pt(3B)–B(4B)–C(1B)	77.0(3)	C(2A)–B(11A)–B(7A)	60.1(5)	C(2B)–B(11B)–B(7B)	59.9(4)
Pt(3A)–B(4A)–B(8A)	65.3(3)	Pt(3B)–B(4B)–B(8B)	66.7(3)	B(6A)–B(11A)–B(10A)	59.0(5)	B(6B)–B(11B)–B(10B)	59.9(5)
C(1A)–B(4A)–B(5A)	57.4(4)	C(1B)–B(4B)–B(5B)	55.9(4)	B(10A)–B(11A)–B(12A)	59.9(6)	B(10B)–B(11B)–B(12B)	59.5(5)
C(1A)–B(4A)–B(8A)	109.2(5)	C(1B)–B(4B)–B(8B)	106.7(5)	B(7A)–B(11A)–B(12A)	60.6(5)	B(7B)–B(11B)–B(12B)	60.8(5)
B(5A)–B(4A)–B(9A)	58.4(4)	B(5B)–B(4B)–B(9B)	59.2(4)	Pt(3A)–B(7A)–C(2A)	68.3(3)	Pt(3B)–B(7B)–C(2B)	79.3(3)
B(8A)–B(4A)–B(9A)	58.7(4)	B(8B)–B(4B)–B(9B)	59.4(4)	Pt(3A)–B(7A)–B(8A)	66.3(3)	Pt(3B)–B(7B)–B(8B)	66.3(3)
C(1A)–B(5A)–B(4A)	56.6(4)	C(1B)–B(5B)–B(4B)	60.6(4)	C(2A)–B(7A)–B(8A)	102.3(5)	C(2B)–B(7B)–B(8B)	108.8(5)
C(1A)–B(5A)–B(6A)	59.2(5)	C(1B)–B(5B)–B(6B)	60.3(5)	C(2A)–B(7A)–B(11A)	59.7(5)	C(2B)–B(7B)–B(11B)	55.9(4)
B(4A)–B(5A)–B(9A)	59.1(4)	B(4B)–B(5B)–B(9B)	60.1(4)	B(8A)–B(7A)–B(12A)	59.5(5)	B(8B)–B(7B)–B(12B)	57.9(5)
B(6A)–B(5A)–B(10A)	60.1(5)	B(6B)–B(5B)–B(10B)	58.1(5)	B(11A)–B(7A)–B(12A)	59.7(5)	B(11B)–B(7B)–B(12B)	59.9(5)
B(8A)–B(5A)–B(10A)	61.9(5)	B(8B)–B(5B)–B(10B)	59.6(5)	B(8A)–B(12A)–B(9A)	60.2(5)	B(8B)–B(12B)–B(9B)	60.6(5)
C(1A)–B(6A)–C(2A)	53.8(4)	C(1B)–B(6B)–C(2B)	51.9(4)	B(8A)–B(12A)–B(7A)	61.3(5)	B(8B)–B(12B)–B(7B)	60.9(5)
C(1A)–B(6A)–B(5A)	58.9(5)	C(1B)–B(6B)–B(5B)	56.7(4)	B(9A)–B(12A)–B(10A)	62.2(5)	B(9B)–B(12B)–B(10B)	60.5(5)
C(2A)–B(6A)–B(11A)	57.9(5)	C(2B)–B(6B)–B(11B)	57.5(5)	B(10A)–B(12A)–B(11A)	60.4(6)	B(10B)–B(12B)–B(11B)	59.0(5)
B(5A)–B(6A)–B(10A)	60.7(5)	B(5B)–B(6B)–B(10B)	61.5(5)	B(11A)–B(12A)–B(7A)	59.7(5)	B(11B)–B(12B)–B(7B)	59.3(5)

C(1) atom in [1-Ph-3,3-$(PMe_2Ph)_2$-*closo*-3,1,2-$PtC_2B_9H_{10}$] **6** could be the cause of a distortion in the bonding between platinum and the C_2B_3 face of the carbaborane ligand. It is now seen that a similar PtC_2B_3 configuration exists in unsubstituted **3A** and therefore the previous suggestion is probably incomplete or perhaps incorrect. The Pt–C and Pt–B distances in **6**, *i.e.* Pt–$C(1)_{Ph}$ 2.596(10), Pt–C(2) 2.326(10), Pt–B(4) 2.313(12), Pt–B(7) 2.257(12) and Pt–B(11) 2.239(12) Å, show a similar pattern to those found in **3A** (Table 3) which has no substituent on either of the carbon atoms of the cage.

The conformation of the PtP_2 unit above the CB_4 face of [2,2-$(PMe_2Ph)_2$-*closo*-2,1,8-$PtC_2B_9H_{11}$] **5** approximates closely to the minimum-energy conformer proposed[6] from a frontier-molecular-orbital analysis (see **IIc** and Fig. 4). This conformation has been described[6] as 'perpendicular' and several similarly configured systems involving ML_2 units above XB_4 faces, specifically where X = Se and Te, have been reported.[4,5] A similar conformation occurs in the sulfur analogue **2** (Fig. 2).

Details of the structure of [2,2-$(PMe_2Ph)_2$-*closo*-2,1-$PtSB_{10}H_{10}$] **2** (Fig. 2 and Table 2) are remarkably similar to those of [2,2-$(PEt_3)_2$-*closo*-2,1-$PtXB_{10}H_{10}$] where X = Se **8**[4] or Te **9**[5] except for the differences expected as a result of the increases in the covalent radius of X with the increase in its atomic number. Within the $\{PtXB_{10}\}$ cages of **2**, **8** and **9** the corresponding B–B and Pt–B distances are very similar. The B–B distances in **2** range from 1.750(5) Å for B(5)–B(9) to 1.938(5) Å for B(5)–B(6). The shortest and longest B–B distances in **8** are also between B(5)–B(9) and B(5)–B(6) respectively at 1.71(3) and 1.96(3) Å. For **9** the shortest distance is B(4)–B(9) at 1.728(12) Å, although B(5)–B(9) is also short at 1.747(12) Å and the longest distance is again B(5)–B(6) at 1.948(13) Å. In each of compounds **2**, **8** and **9** the mean value of the two X-flanked Pt–B distances, Pt–B(3) and Pt–B(6), is slightly greater than the mean of the Pt–B(7) and Pt–B(11) distances. The pairs of values are 2.307 and 2.239, 2.30 and 2.25, and 2.294 and 2.250 Å, respectively. The expected increase in X–B distances as X is changed through the sequence S, Se to Te is observed. The mean

Table 4 Selected interatomic distances (Å) and angles (°) for [2,2-$(PMe_2Ph)_2$-*closo*-2,1,8-$PtC_2B_9H_{11}$] **5** with e.s.d.s in parentheses

Pt(2)–P(1)	2.2891(6)	B(7)–B(12)	1.766(4)	B(4)–B(9)	1.755(5)	P(2)–C(6)	1.814(3)
Pt(2)–B(3)	2.233(3)	B(9)–B(10)	1.774(5)	B(5)–B(10)	1.770(6)	C(1)–B(4)	1.644(4)
Pt(2)–B(11)	2.223(3)	B(10)–B(12)	1.749(5)	B(7)–C(8)	1.707(4)	B(3)–B(4)	1.840(4)
P(1)–C(11)	1.819(3)	Pt(2)–P(2)	2.2972(6)	C(8)–B(9)	1.725(4)	B(4)–B(5)	1.726(5)
P(2)–C(21)	1.822(2)	Pt(2)–B(6)	2.273(3)	B(9)–B(12)	1.759(5)	B(5)–B(6)	1.820(5)
C(1)–B(5)	1.662(4)	P(1)–C(3)	1.817(3)	B(11)–B(12)	1.758(4)	B(6)–B(10)	1.781(5)
B(3)–B(7)	1.873(4)	P(2)–C(5)	1.821(3)	Pt(2)–C(1)	2.570(3)	B(7)–B(11)	1.796(4)
B(4)–C(8)	1.722(4)	C(1)–B(3)	1.674(4)	Pt(2)–B(7)	2.215(3)	C(8)–B(12)	1.702(4)
B(5)–B(9)	1.749(5)	C(1)–B(6)	1.678(5)	P(1)–C(4)	1.807(3)	B(10)–B(11)	1.755(5)
B(6)–B(11)	1.881(5)	B(3)–C(8)	1.746(4)				
P(1)–Pt(2)–P(2)	97.43(2)	C(1)–Pt(2)–B(3)	40.02(10)	B(10)–B(6)–B(11)	57.19(18)	Pt(2)–B(7)–B(11)	66.38(13)
C(1)–Pt(2)–B(6)	39.95(11)	B(6)–Pt(2)–B(11)	49.46(12)	B(3)–B(7)–B(11)	103.21(19)	B(3)–B(7)–C(8)	58.17(15)
B(3)–Pt(2)–B(7)	49.81(10)	Pt(2)–C(1)–B(3)	59.06(12)	B(11)–B(7)–B(12)	59.14(17)	C(8)–B(7)–B(12)	58.69(17)
B(7)–Pt(2)–B(11)	47.73(11)	B(3)–C(1)–B(4)	67.38(18)	B(3)–C(8)–B(7)	65.69(16)	B(3)–C(8)–B(4)	64.09(17)
Pt(2)–C(1)–B(6)	60.42(12)	B(3)–C(1)–B(6)	105.08(19)	B(4)–C(8)–B(9)	61.22(19)	B(7)–C(8)–B(12)	62.39(17)
B(4)–C(1)–B(5)	62.97(20)	Pt(2)–B(3)–C(1)	80.93(14)	B(9)–C(8)–B(12)	61.75(19)	B(4)–B(9)–B(5)	59.03(21)
B(5)–C(1)–B(6)	66.04(20)	Pt(2)–B(3)–B(7)	64.60(12)	B(4)–B(9)–C(8)	59.32(18)	C(8)–B(9)–B(12)	58.50(18)
C(1)–B(3)–B(7)	113.08(20)	C(1)–B(3)–B(4)	55.54(16)	B(5)–B(9)–B(10)	60.31(21)	B(5)–B(10)–B(6)	61.66(19)
B(7)–B(3)–C(8)	56.14(15)	B(4)–B(3)–C(8)	57.32(16)	B(10)–B(9)–B(12)	59.36(20)	B(9)–B(10)–B(12)	59.90(20)
C(1)–B(4)–B(5)	59.02(19)	C(1)–B(4)–B(3)	57.09(16)	B(5)–B(10)–B(9)	59.16(20)	Pt(2)–B(11)–B(6)	66.64(13)
B(3)–B(4)–C(8)	58.59(16)	B(5)–B(4)–B(9)	60.32(21)	B(6)–B(10)–B(11)	64.27(18)	B(6)–B(11)–B(7)	103.43(19)
C(8)–B(4)–B(9)	59.46(18)	C(1)–B(5)–B(4)	58.01(19)	B(11)–B(10)–B(12)	60.21(19)	B(7)–B(11)–B(12)	59.59(17)
C(1)–B(5)–B(6)	57.41(17)	B(6)–B(5)–B(10)	59.48(20)	Pt(2)–B(11)–B(7)	65.88(12)	B(7)–B(12)–C(8)	58.92(16)
B(4)–B(5)–B(9)	60.65(20)	Pt(2)–B(6)–C(1)	79.62(15)	B(6)–B(11)–B(10)	58.54(18)	C(8)–B(12)–B(9)	59.74(19)
B(9)–B(5)–B(10)	60.52(21)	C(1)–B(6)–B(5)	56.54(19)	B(10)–B(11)–B(12)	59.73(19)	B(7)–B(12)–B(11)	61.28(17)
Pt(2)–B(6)–B(11)	63.90(12)	C(1)–B(6)–B(11)	112.57(20)	B(10)–B(12)–B(11)	60.07(19)	B(9)–B(12)–B(10)	60.74(20)
B(5)–B(6)–B(10)	58.86(20)	Pt(2)–B(7)–B(3)	65.59(12)				

values of the Pt-flanked X–B(3) and X–B(6) distances are larger than those of the X–B(4) and X–B(5) distances. The pairs of values are 2.047 and 1.976, 2.19 and 2.09, and 2.400 and 2.305 Å, respectively. The Pt–X distances increase in the sequence Pt–S 2.6633(7), Pt–Se 2.676(2) and Pt–Te 2.704(1) Å, as expected. The two Pt–P distances in **2**, 2.2870(7) and 2.3021(7) Å, differ more than the corresponding distances in either **8** or **9**, but the magnitude of this difference is not unusual in platinum phosphine complexes in general where there is no crystallographic plane of symmetry through Pt.

NMR Spectroscopy of compounds 1–3 and 5

The ^{11}B, ^{11}B-$\{^1H\}$, ^1H and ^1H-$\{^{11}B\}$ NMR spectra of the platinadiarsenaborane **1** are consistent with the molecular constitution (Fig. 1). The configuration in Fig. 1 is asymmetric, but compound **1** exhibits a 1:1:2:2:2:1 intensity pattern in the ^{11}B-$\{^1H\}$ spectrum. This, however, is exactly analogous to the intensity patterns of the previously reported compounds [3,3-L_2-*closo*-3,1,2-$PtAs_2B_9H_9$] where L = PPh_3 or PMe_2Ph.[3] The ^1H spectrum of **1** contains a triplet centred at δ +1.21 and a quartet centred at δ +2.10 which are assigned to the CH_3 and CH_2 protons on the triethylphosphine ligands. Clearly, both the ^{11}B-$\{^1H\}$ and ^1H spectra indicate that, in solution, the phosphine ligands are, on time-averaging, equivalent and hence that the $\{Pt(PEt_3)_2\}$ unit is freely rotating about a pseudo-axis passing through Pt(3) and B(10), with the $As_2B_9H_9$ ligand displaying a time-averaged mirror-plane symmetry.

Multinuclear NMR spectroscopy (^{11}B, ^{11}B-$\{^1H\}$, ^{31}P, ^{195}Pt and ^1H) was used to characterise [3,3-$(PMe_2Ph)_2$-*closo*-3,1,2-$PtC_2B_9H_{11}$] **3**. There were six peaks in the ^{11}B-$\{^1H\}$ spectrum with an intensity pattern 1:1:2:2:1:2, and six corresponding ^1H resonances. Assignments were made by relative intensities, incidence of ^{195}Pt satellites, [^{11}B–^{11}B] correlation spectroscopy (COSY), and ^1H-$\{^{11}B\}$ selective experiments. The ^{11}B shielding pattern can be traced to those of *closo*-1,2-$C_2B_{10}H_{12}$ or other *closo*-MC_2B_9 clusters, *e.g.* [3-(η^5-C_5Me_5)-*closo*-3,1,2-$IrC_2B_9H_{11}$] (Fig. 5).[15] In the comparisons of both $C_2B_{10}H_{12}$ and the 3,1,2-$IrC_2B_9H_{11}$ compound with **3** the greatest differences are in the 8 and 4,7 positions, *i.e.* those adjacent to platinum. Of these, only the $^{11}B(8)$ shift deviation for compound **3** is particularly marked. The other ^{11}B resonances are within a *ca.* 10 ppm range which is typical of a compact, twelve-vertex *closo*-carbaborane pattern. As with [3-(η^5-C_5Me_5)-*closo*-3,1,2-$IrC_2B_9H_{11}$] there is no particularly marked similarity of shielding patterns between the $\{C_2B_9H_{11}\}$ fragment and either neutral $C_2B_9H_{13}$ or the $[C_2B_9H_{12}]^-$ anion. Therefore, in contrast, for example, to the $PtC_2B_8H_{10}$ system,[16] no clear idea can be obtained from consistency in NMR shielding patterns as to which, based on a time average,

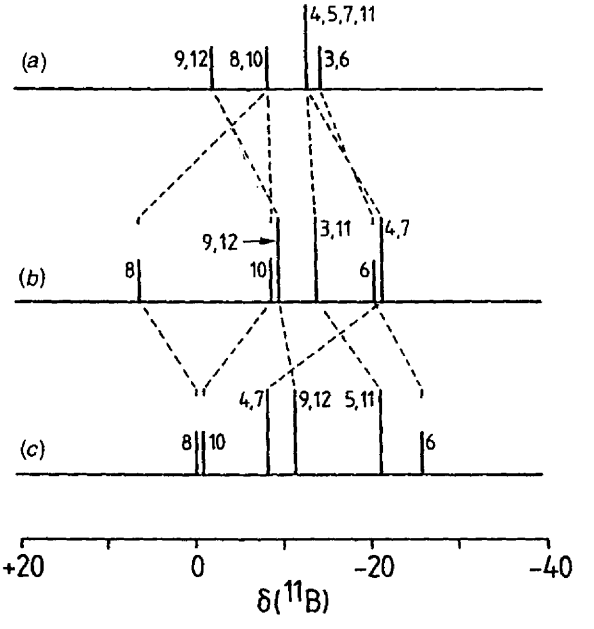

Fig. 5 Correlation diagram for ^{11}B NMR data for (*a*) *closo*-1,2-$C_2B_{10}H_{12}$, (*b*) [3,3-$(PMe_2Ph)_2$-*closo*-3,1,2-$PtC_2B_9H_{11}$] **3**, and (*c*) [3-(η^5-C_5Me_5)-*closo*-3,1,2-$IrC_2B_9H_{11}$] with dashed lines showing the equivalent positions in each species

is the most stable of the different metal-to-heteroborane ligand conformations. The ^{1}H NMR shielding when plotted against the ^{11}B shielding also falls into established *closo* patterns with a fairly steep gradient $\delta(^{11}B)/\delta(^1H)$ of 11. The somewhat higher shielding of ^{1}H(6), as compared to the general trend, is also found for the compounds $[\{LM\}C_2B_9H_{11}]$ where LM = $(\eta^5$-$C_5Me_5)Rh$, $(\eta^5$-$C_5Me_5)Ir$ or $(\eta^6$-$C_6Me_6)Ru$.[17,18] In **3** the much lower shielding of ^{1}H(10), which is antipodal to platinum, has precedent in other previously examined *closo* systems.[3,19] Cluster atoms such as Pt and Ir generally induce anomalously low antipodal ^{1}H shieldings in twelve-vertex *closo* and some other clusters.[3,17,20]

The existence of a single asymmetric conformer of the platinadicarbaborane **3** in solution is excluded on the basis of the ^{31}P NMR behaviour, which showed only one resonance down to 183 K, and the ^{1}H NMR also precludes a symmetric static single conformer, there being only one PMe_2Ph methyl resonance down to 163 K. A static symmetrical structure would engender two PMe ^{1}H resonances,[4,21] and a static asymmetric one would engender four.[22] The possibility of accidental coincidence of two (or more) PMe ^{1}H chemical shifts at the variety of temperatures encountered is unlikely, since, at all temperatures used, only one resonance was observed in two solvents of widely different polarities and anisotropies, namely CD_2Cl_2 and $CD_3C_6D_5$. The value of $\Delta G^\ddagger$ for the fluxional process involving the $Pt(PMe_2Ph)_2$ unit in **3** rotating above the C_2B_3 face to which it is attached is therefore estimated to be < 30 kJ mol^{-1}. This is an upper limit and the actual value is possibly somewhat less if the broadening observed at 163 K (supercooled CD_2Cl_2 solution) arises from solution relaxation effects rather than incipient cessation of the fluxionality. This small energy difference, which is the maximum difference between *any* two rotamers (eclipsed or non-eclipsed), is of a similar magnitude to that of crystal-packing forces.

The NMR parameters for the ^{11}B, ^{31}P and ^{1}H nuclei in [2,2-$(PMe_2Ph)_2$-*closo*-2,1,8-$PtC_2B_9H_{11}$] **5** were also measured to characterise this compound. The ^{11}B-$\{^1H\}$ spectrum consisted of nine different resonances, each of unit relative intensity, in the region $\delta(^{11}B)$ −7.6 to −24.2 and each boron has one hydrogen atom attached as determined by ^{1}H-$\{^{11}B\}$ experiments. At low temperatures the PMe protons exhibited four resonances, implying a static asymmetric structure.[22] At higher temperatures each of the two pairs coalesced to give one resonance, with a coalescence temperature of 272 K for the 100 MHz spectrum in $CDCl_3$ solution. This yielded a value for $\Delta G^\ddagger$ of *ca.* 58 kJ mol^{-1} for the rotational process in **5**.[2]

Compound **2**, [2,2-$(PMe_2Ph)_2$-*closo*-2,1-$PtSB_{10}H_{10}$], was also examined by NMR spectroscopy, assignments being made by incidence of ^{195}Pt satellites, relative intensities and comparisons of shifts and linewidths with those of the previously reported selenium[4] and tellurium[5] analogues. The ^{11}B NMR spectrum exhibited a 2:2:2:2:1:1 relative intensity pattern, implying a static symmetrical structure or rapid equilibration among asymmetric forms. Below room temperature two PMe ^{1}H resonances are observed implying a symmetric static structure,[5,21] whereas at higher temperatures these two coalesce. The observed coalescence temperature of 289 K (100 MHz ^{1}H spectrum, $CDCl_3$ solvent) gives $\Delta G^\ddagger$ of *ca.* 61 kJ mol^{-1} for the rotation of the $Pt(PMe_2Ph)_2$ unit above the SB_4 face.

The assigned NMR spectrum of compound **2** now permits a comparison of the ^{11}B and ^{1}H shielding trends for the short series of analogues [2,2-$(PMe_2Ph)_2$-*closo*-2,1-$PtXB_{10}H_{10}$] where X is S, Se or Te, Fig. 6. It can be deduced from the very close ^{11}B shielding parallels (lower diagrams) that the electronic structures are very similar and the similarities thereby also suggest very similar rotamer populations for all three compounds in solution. In the plot of $\delta(^1H)$ *versus* $\delta(^{11}B)$ for the various BH units there is an approximately linear correlation, with lower-field ^{11}B resonances tending to be

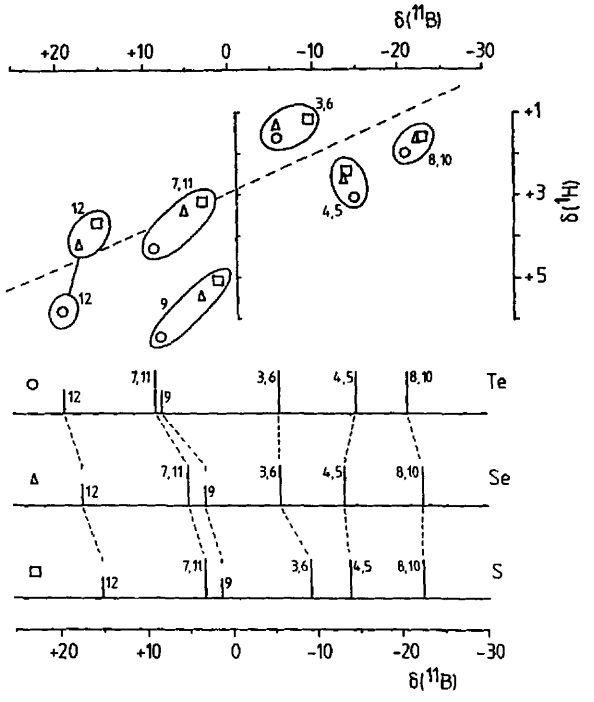

Fig. 6 Cluster ^{11}B and ^{1}H NMR data for compounds [2,2-$(PMe_2Ph)_2$-*closo*-2,1-$PtXB_{10}H_{10}$] [X = S **2** (□), Se (△) or Te (○)]. The top diagram is a plot of $\delta(^1H)$ *versus* $\delta(^{11}B)$ for the individual BH cluster units, and the bottom one is a correlation diagram for ^{11}B chemical shifts

associated with lower-field ^{1}H resonances, but there is considerable deviation from a straight line. Noteworthy again are the considerably lower ^{1}H shieldings for hydrogen atoms antipodal to the heavy atoms,[3,17,20] specifically for the BH(9) data for all three compounds [antipodal to Pt(2)], and for the BH(12) datum for the tellurium compound [antipodal to Te(1)].

The shift–twist mechanism

The free-energy barriers to rotation reported previously for a number of $Pt(PMe_2Ph)_2$ derivatives of heteroboranes are collected together with the present datum for **2** and related data for palladium derivatives in Table 5. Values of $\Delta G^\ddagger$ range from < 30 to 62 kJ mol^{-1} and for these particular compounds fall into two groups according to geometry of the face of heteroborane ligand to which the metal atom is bonded, *i.e.* either X_2B_3 or XB_4. The barriers to rotation above XB_4 ligand faces (X = C, S, Se or Te) are significantly higher (by a factor of *ca.* 2) than those above X_2B_3-faced ligands which have the X atoms adjacent (X = C or As). Whilst it could be suggested that there should be a contribution to the barrier to rotation which is related to the size of X in an XB_4 face (see Table 5 for data from X = C, S, Se or Te), there are clearly other (electronic) factors involved. The combined effects of size and electronic influence of X are also unclear in the data for the X_2B_3-faced ligands since the $\Delta G^\ddagger$ values are indistinguishable for X = C and As. It is apparent that, in the solid-state structures established so far, compounds which exhibit more than one conformer *e.g.* **1** and **3** (see Table 5 for the analogous PMe_2Ph compounds), have rotational free-energy barriers that are low, whereas those with single-conformer structures, *e.g.* **2**, **5** and [2,2-$(PMe_2Ph)_2$-2,1-$PtXB_{10}H_{10}$] (X = Se or Te), have high barriers. However, generalisations from this limited set of compounds and structures should be made with care. The $\Delta G^\ddagger$ values measured are for the complete exchange of the PMe_2 sites, *i.e.* for a complete 180° half-rotation of the $Pt(PMe_2Ph)_2$ unit above the heteroborane ligand. In the XB_4-faced ligands there will be a succession of rotational maxima and minima (see Discussion

Table 5 Free energies of the barrier to rotation of ML_2 units in twelve-atom *closo*-metallaheteroboranes

Compound[a]	Coalescence temperature/K	$\Delta G^{\ddagger}_{T}$/kJ mol^{-1}	Ref.
[2,2-L_2-2,1,8-$PtC_2B_9H_{11}$]	272	57.8 ± 1.2	2
[2,2-L_2-2,1-$PtSB_{10}H_{10}$]	289	61.2 ± 1.2	This work
[2,2-L_2-2,1-$PtSeB_{10}H_{10}$]	328	*ca.* 58	4
[2,2-L_2-2,1-$PtTeB_{10}H_{10}$]	328	62	5
[3,3-L_2-3,1,2-$PtC_2B_9H_{11}$]	< 163[b]	≤30	2
[3,3-L_2-3,1,2-$PtAs_2B_9H_9$]	< 173	≤30	3
[3,3-L_2-3,1,2-$PdAs_2B_9H_9$]	< 183	≤30	3

[a] L = PMe_2Ph. For the cage-substituted compounds [1-Ph-2,2-L_2-2,1-$PtPB_{10}H_{10}$], $\Delta G^{\ddagger}$ = *ca.* 58 kJ mol^{-1} [2,3] and [3-Cl-3,8-L_2-3,1,2-$PdAs_2B_9H_8$], $\Delta G^{\ddagger}_{298}$ = *ca.* 32 kJ mol^{-1}.[3] [b] No coalescence observed even at 163 K.[2]

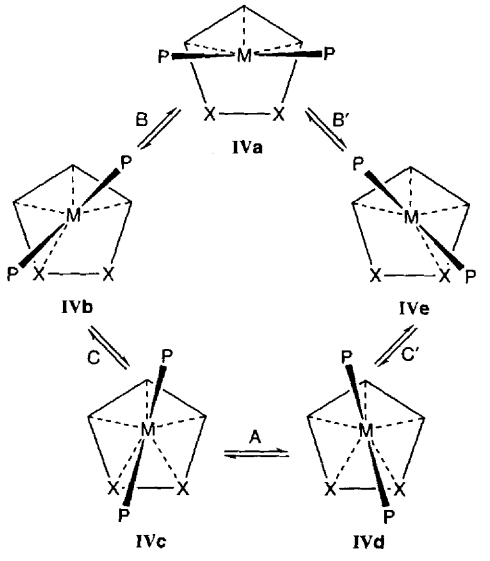

near Fig. 7 below), with one maximum, perhaps that corresponding to the Pt–X/Pt–P eclipse, predominating. The energy differences between the other rotamers will probably be small, and so more than one conformer could be observable in compounds with XB_4-faced ligands. Future work may reveal a rotationally disordered XB_4-faced species.

In any event, the present experimental results permit the following mechanism to be proposed for the rotational process for the X_2B_3-faced ligand species. With identical phosphine ligands, a complete rotation will be characterised by five transition states, one unique (**A**), and two equivalent pairs (**B**, **B'** and **C**, **C'**). These correspond approximately to the successive eclipsing by the Pt–P vector of the vectors from the platinum atom to the five open-face ligand atoms, *i.e.* for example, C_2B_3 or As_2B_3 in **3** or **1** respectively. The intermediates will also exhibit one unique structure, **IVa** which is comparable to **3B**, and two equivalent pairs, **IVb**, comparable to **3A**, and **IVe**, and **IVc** and **IVd**. Each of these intermediates may be observable in a variety of conformers (see **1** and **3** above). The individual steps in the rotation will be typified by the **IVa** ⟷ **IVb** transition. In this, starting from the symmetrical configuration **IVa**, the rotation is initiated by the ML_2 unit shifting from the η^3-bonded system (as in **B**) to an η^4-bonded system. This shift requires that the ML_2 unit begins to twist about the face of the heteroborane ligand to maximise the η^4 ML_2-to-face bonding. This can then either reverse to the starting structure **IVa** or progress to the next minimum **IVc**. As yet there is no experimental evidence as to whether **IVc**/**IVd** are best described as η^5-bonded species or have a reduced hapticity. However, the whole rotation may be visualised as a succession of twists associated with partial detachment and reattachment of the metal atom utilising η^5-, η^4- and η^5-bonding modes rather than as a simple spinning of the PtL_2 moiety about a fixed metal–antipodal boron axis.* The suggested mechanism is similar to those requiring changes in hapticity that have been suggested to explain fluxional behaviour in a number of organometallic compounds.[25]

The proposal illustrated is fully consistent with the data from the crystal and solution studies presented and can be used to explain the general rotational processes for the XB_4-faced compounds as well as the X_2B_3-faced compounds in Table 5. To explain the actual observed differences in free energies of rotation above different X_2B_3- and XB_4-faced ligands would require modelling of the relationship between rotational conformer structure and molecular energy. Studies of this type have recently been reported for the estimation of the minimum-energy conformation of [3,3-L_2-4-SMe_2-3,1,2-$RhC_2B_9H_{10}$] [L_2 = $(CO)_2$ or η^2:η^2-1,5-C_8H_{12}].[26] Clearly, if the rotational process is to be better understood, it will be necessary to take into account the energies of the intermediates in which the metal unit shifts among the η^5-, η^4- and η^3-bonding modes, and also the differences in energy among these and the eclipsed transition states. However, even without exact molecular-energy calculations it is reasonable to predict the general form of the energy-rotation profiles to be as in Fig. 7. In an L_2M–XB_4 system, for example, it is reasonable that the energy maxima correspond to the closest approaches of the M–L vectors of the ML_2 unit to the X and BH units in the XB_4 face [*i.e.* 'eclipsed' conformations encountered as the PtL_2 unit rotates above the XB_4 face as shown in Fig. 7(*a*)]. If this is so, then the energy–rotation profile, Fig. 7(*b*), might be expected to show a series of maxima. Of these, the interaction of PtL_2 with PtX when the PtL_2 unit is rotated by θ = 90° is possibly the largest thus dictating the overall barrier to complete rotation, with the other interactions, *i.e.* PtL_2–BH, requiring less energy to overcome. For a given compound, the precise shape of the profile and the actual maximum and minimum values will depend on individual electronic and steric effects. Similar arguments apply to the X_2B_3-faced compounds. In the solid state, any conformation corresponding to a ΔG value less than a critical value, ΔG^c (which will be dictated by packing forces), will in principle be observable.

Regarding other observed twelve-vertex fluxionalities, a possible relationship exists between the suggested mechanism for the rotational processes discussed above and the *closo* to *exo-nido* rearrangements observed in the chemistry of [{$Rh(PPh_3)_2H$}$C_2R_2B_9H_9$] compounds.[12,13] The η^4 ⟷ η^3 shift, for which direct evidence appears to exist in the crystal

* During the final stages of the preparation of this paper an account of a study of the fluxionality of a related palladium species [3,3-$(PMe_2Ph)_2$-7,8-$(CN)_2$-*closo*-3,1,2-$PdC_2B_9H_9$] was published.[24] The overall NMR results are interpreted in terms of 'some complex exchange process not yet fully understood', and a rotational process of the type that we describe here is discounted. However, the results on the pure compound appear to us to be entirely consistent with an intramolecular rotational fluxionality of the type described here.

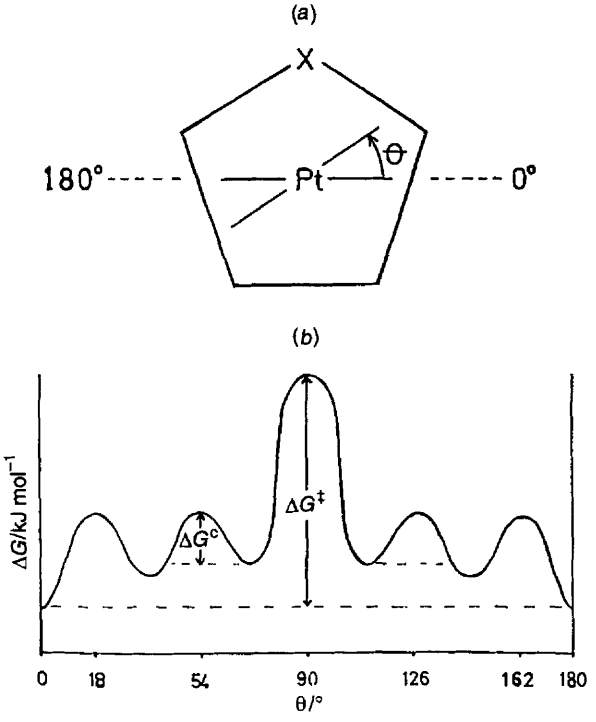

Fig. 7 Energy–rotation profile (*b*) for the $L_2Pt–XB_{10}$ system (*a*)

structure of **3**, and indirect evidence in the rotation of the $M(PMe_2Ph)_2$ units, may well constitute part of the process which leads to the removal of $Rh(PPh_3)_2$ units from the cluster apex positions in $[3,3\text{-}(PPh_3)_2\text{-}3\text{-}H\text{-}closo\text{-}3,1,2\text{-}RhC_2R_2B_9H_9]$ complexes to afford the isomeric $[exo\text{-}(Ph_3P)_2Rh\text{-}nido\text{-}7,8\text{-}C_2R_2B_9H_{10}]$ compounds. Hawthorne and co-workers[13] noted that the formation of the *exo-nido* compounds occurred *via* the reduction in co-ordination of the rhodium atom from (η^5-C_2B_3)Rh to (η^1-facial BH)Rh with concomitant formation of a B–H–B bridge on the face of the evolving $[nido\text{-}C_2R_2B_9H_{10}]^-$ ligand. Details of this process were not specified but it was suggested on the basis of molecular-modelling calculations that 'no viable *endo-nido*-Rh(1+) tautomer based upon a dicarbollide ligand of variable hapticity can exist in other than the guise of a transition state for *closo–exo-nido* tautomerization'. It now seems possible that the reduction in co-ordination of rhodium could indeed proceed from η^5 through η^4-, η^3- and even η^2-C_2B_3 face-bonded rhodium intermediates leading to the Rh–H–B-containing intermediate considered by Hawthorne. There are now several examples in the literature of fluxional processes which are suggested to involve a change in metal-to-cage hapticity with concomitant transfer of a bridging H atom between two equivalent B–B sites. One such is the interchange of eleven-vertex *nido*-structured enantiomeric forms of $[8,8\text{-}(PPh_3)_2\text{-}8,7\text{-}RhSB_9H_{10}]$,[27] and closely related to this is the analogous dynamic enantiomerisation of $[8,8\text{-}(PMe_2Ph)_2\text{-}8,7\text{-}PtCB_9H_{10}]$.[22] In the case of the platinum compounds in the present study it may well be that the impossibility of the formation of a B–H–B bond in any *exo-nido* compounds derived from $[\{Pt(PR_3)_2\}C_2B_9H_{11}]$ is one of the features that preclude *closo* to *exo-nido* tautomerisation. On the other hand, although *exo* co-ordination of PtL_2 units to polyhedral borane and carbaborane ligands has some precedent, known compounds tend to be unstable.[28,29]

Experimental

General

All syntheses of reagents, purification of solvents, manipulative procedures (except those using microwave heating), apparatus and techniques for recording spectra used have been described in previous Parts of this series.[1] Microwave-initiated reactions were performed in a modified Ariston model MW 950 TW domestic microwave oven which has a maximum power setting of 650 W. Reactions were carried out in a thick-walled glass tubular vessel (25 cm long, 3.5 cm diameter) as described by Baghurst and Mingos.[14] The pressure-measuring system was based on a Druck PDCR 810-0799, 0–35 bar (bar = 10^5 Pa) pressure transducer. This and the associated pressure indicator were from RS Components, Corby, Northants. The compounds *cis*-$[PtCl_2(PMe_2Ph)_2]$, *cis*-$[PtCl_2(PEt_3)_2]$,[30] $Cs[7,8\text{-}C_2B_9H_{12}]$,[31] $NMe_4[7,8\text{-}As_2B_9H_{10}]$[32] and $SB_{10}H_{12}$[33] were prepared according to literature methods. The NMR spectroscopy was carried out as described in earlier papers[4,5,17–19] with chemical shifts δ quoted in ppm to low frequency (high field) of Ξ 100 MHz for ^1H ($SiMe_4$), Ξ 40.480 730 MHz for ^{31}P (nominally 85% H_3PO_4), Ξ 32.083 971 MHz for ^{11}B ($F_3B{\cdot}OEt_2$) and Ξ 21.4 MHz for ^{195}Pt (arbitrary standard, the 'Goodfellow scale'),[34] Ξ being defined as in ref. 35. The splittings $N(^{31}P–^1H)$ quoted are $^2J(^{31}P–C–^1H) + {}^4J(^{31}P–Pt–P–C–^1H)$.

Syntheses

$[3,3\text{-}(PEt_3)_2\text{-}closo\text{-}3,1,2\text{-}PtAs_2B_9H_9]$ 1. A mixture of $NMe_4[7,8\text{-}As_2B_9H_{10}]$ (0.100 g, 0.30 mmol) in ethanol (20 cm^3), triethylamine (0.4 cm^3, 3.0 mmol) and *cis*-$[PtCl_2(PEt_3)_2]$ (0.15 g, 0.30 mmol) in ethanol (10 cm^3) was introduced into a thick-walled glass reaction vessel (25 cm long, 3.5 cm diameter). The mixture was subjected to microwave irradiation (650 W) for 8 min. The red solution was filtered and the solvent removed under reduced pressure (rotary evaporator, 35 °C). The residue was dissolved in CH_2Cl_2 and subjected to preparative TLC with CH_2Cl_2–heptane (4:1) as liquid phase. One major product was isolated and recrystallised from CH_2Cl_2–heptane (4:1) as red crystals of $[3,3\text{-}(PEt_3)_2\text{-}closo\text{-}3,1,2\text{-}PtAs_2B_9H_9]$ **1** (0.135 g, 64.5%) (Found: C, 21.20; H, 6.00. $C_{12}H_{39}As_2B_9P_2Pt$ requires C, 20.95; H, 5.70%). IR: ν_{max}(KBr) 2529vs and 2496s (sh) cm^{-1} (BH). $^{11}B\text{-}\{^1H\}$ and $^1H\text{-}\{^{11}B\}$ NMR {$CDCl_3$, 294–298 K; ordered as $\delta(^{11}B)$; assignment, $^1J(^{11}B–^1H)$/Hz [$\delta(^1H)$]}: +12.8, B(8) [+3.89]; +5.8, B(10) [+6.19]; +1.5, B(9,12) [+3.56]; +1.5, B(4,7) [+2.11]; −13.1, B(5,11) [+2.85] and −16.2, B(6) [+2.77].

$[2,2\text{-}(PMe_2Ph)_2\text{-}closo\text{-}2,1\text{-}PtSB_{10}H_{10}]$ 2. The complex $[PtCl_2(PMe_2Ph)_2]$ (0.100 g, 0.18 mmol) was added to a solution of *nido*-7-$SB_{10}H_{12}$ (0.031 g, 0.20 mmol) and 'proton sponge' (0.077 g, 0.36 mmol) in CH_2Cl_2 (20 cm^3). The colourless mixture was stirred for 7 h at room temperature during which time a yellow colour developed. The mixture was filtered through silica and the silica washed with CH_2Cl_2 (20 cm^3). The filtrate was concentrated and applied to preparative TLC plates (silica gel G, Fluka GF 254). Development with CH_2Cl_2–heptane (1:1) yielded one mobile component (R_f 0.9). Extraction with CH_2Cl_2 followed by evaporation afforded a pale yellow compound which was identified as $[2,2\text{-}(PMe_2Ph)_2\text{-}closo\text{-}2,1\text{-}PtSB_{10}H_{10}]$ **2** (0.012 g, 11%). $^{11}B\text{-}\{^1H\}$ and $^1H\text{-}\{^{11}B\}$ NMR {$CDCl_3$, 294–298 K; ordered as $\delta(^{11}B)$, assignment, [$\delta(^1H)$]}: +15.6, B(12) [+3.70]; +3.3, B(7,11) [+3.14]; +1.69, B(9) [+5.07]; −9.1, B(3,6) [+1.18]; −13.6, B(4,5) [+2.42] and −22.5, B(8,10) [+1.59]. Additionally, $^1J(^{11}B–^1H)$ Hz for BH(12) 128 ± 5 and for BH(8,10) 138 ± 5 (others not measurable because of the broadness of peaks), $^1J(^{195}Pt–^{11}B)$ for B(7,11) = 225 and $^3J(^{195}Pt–^1H)$ for BH(12) = 62 Hz. ^{31}P NMR (CD_2Cl_2, *ca.* 150 K): δ −10.7 [$^1J(^{195}Pt–^{31}P)$ 3108 ± 2 Hz]. Additionally, $\delta(^1H)$ (PMe) [*N*/Hz, $^3J(^{195}Pt–^1H)$/Hz] +1.81 [10.2, 23.0] and +1.53 [10.3, 32.7] at low temperatures; coalesced at 257 K (100 MHz spectrum) ($\Delta G^‡$ 61.2 ± 1.2 kJ mol^{-1}) to give δ +1.69 at 295 K.

Table 6 Summary of crystal data, data collection, structure solution and refinement details for compounds **1** and **2**[a]

	1	**2**
(*a*) Crystal data		
Empirical formula	$C_{12}H_{39}As_2B_9P_2Pt$	$C_{16}H_{32}B_{10}P_2PtS$
M	687.6	621.6
Colour, habit	Red, needle	Yellow
Crystal size/mm	0.51 × 0.18 × 0.10	0.53 × 0.38 × 0.30
Space group	*Cc*	$P2_1/c$
a/Å	10.5014(13)	11.8372(10)
b/Å	17.2554(16)	9.9542(10)
c/Å	14.433(3)	21.709(2)
β/°	106.366(12)	99.132(9)
U/Å^3	2509.3(6)	2525.5(2)
F(000)	1320	1208
D_c/g cm^{-3}	1.820	1.635
μ/mm^{-1}	8.39	5.57
(*b*) Data acquisition[b]		
Maximum θ/° for reflections	26.9	25.0
Reflections measured	2832	8992
Unique reflections	2832	4446
R_{int}	—	0.0285
Reflections with $I > n\sigma(I)$, *n*	2574, 3.0	4173, 2.0
Minimum, maximum absorption correction	0.0810, 0.1912	0.5071, 0.8347
(*c*) Structure solution and refinement[c]		
Refinement on	*F*	F^2
Hydrogen atom treatment	Riding	BH refined, others riding
No. variables	240	316
Weights: either		
k in $w = 1/[\sigma^2(F_o) + kF_o^2]$		0.0002
or $w = 1/[\sigma^2(F_o^2) + k]$		0.015
$P = (F_o^2 + 2F_c^2)/3$		1.2122
R, *R*′, goodness of fit	0.017, 0.021, 1.03	0.018, 0.042, 1.09
Density range in final Δ map/e Å^{-3}	−0.46, 0.48	−0.38, 0.51
Final shift/error ratio	0.003	0.001
Secondary extinction type	Larson[37]	SHELXL 93[40]
Secondary extinction correction	0.024(10)	0.0060(5)

[a] Details in common: monoclinic; $Z = 4$; 293 K; absorption correction by ψ scans: Patterson heavy-atom method. [b] Data collection (with graphite-monochromatised Mo-Kα radiation) on an Enraf-Nonius CAD4 diffractometer for compound **1** and a Stoe STADI4 diffractometer for **2** (using the line-profile method[38]). [c] All calculations were done with the NRCVAX system of programs[39] for refinement on *F* with observed data (compound **1**), or with SHELXL 93[40] for refinement on F^2 with all data (compound **2**). Occupancy factors for partially occupied As/B positions: As(1) 0.8346, As(2) 0.7857, B(4) 0.2592, B(7) 0.2385 and B(8) 0.2161.

[3,3-(PMe$_2$Ph)$_2$-*closo*-3,1,2-PtC$_2$B$_9$H$_{11}$] 3 and [2,2-(PMe$_2$Ph)$_2$-*closo*-2,1,8-PtC$_2$B$_9$H$_{11}$] 5. *Procedure* (*a*), *reaction with microwave-induced heating*. A mixture of Cs[7,8-C$_2$B$_9$H$_{12}$] (0.100 g, 0.376 mmol), ethanol (20 cm^3), triethylamine (0.38 g, 3.76 mmol) and *cis*-[PtCl$_2$(PMe$_2$Ph)$_2$] (0.204 g, 0.376 mmol) was introduced into a thick-walled glass reaction vessel (25 cm long, 3.5 cm diameter). The mixture was subjected to microwave irradiation (650 W) for 30 min in a modified microwave apparatus described elsewhere.[8,14] The dark yellow solution was filtered and the solvent removed under reduced pressure (rotary evaporator, 35 °C). The residue was dissolved in CH_2Cl_2 and subjected to preparative TLC with CH_2Cl_2–hexane (3:2) as eluent. Two major products were isolated. One ($R_f = 0.65$) was recrystallised from CH_2Cl_2–hexane (3:2) as colourless crystals of [2,2-(PMe$_2$Ph)$_2$-*closo*-2,1,8-PtC$_2$B$_9$H$_{11}$] **5** (0.044 g, 19.4%) (Found: C, 36.2; H, 5.90. C$_{18}$H$_{33}$B$_9$P$_2$Pt requires C, 35.8; H, 5.50%). IR: ν_{max}(KBr) 2555vs, 2518vs, 2497s (sh) and 2458s cm^{-1} (BH). ^{11}B-{^{1}H} and ^{1}H-{^{11}B} NMR {CDCl$_3$, 294–298 K; ordered as δ(^{11}B), multiplicity, intensity, $^1J(^{11}B-^1H)$/Hz, [δ(^{1}H)]}: −7.6, s, 1B, 154 ± 5 [+2.53]; −9.4, s, 1B, 129 ± 5 [+1.73]; −9.9, s, 1B, 129 ± 5 [+2.24]; −12.1, s, 1B, 158 ± 5 [+4.11]; −15.7, s, 1B, 138 ± 5 [+1.38]; −20.5, s, 1B, 167 ± 5 [+1.87]; −21.8, s, 1B, 172 ± 5 [+2.24]; −22.8, s, 1B, 173 ± 5 [+1.41] and −24.2, s, 1B, 143 ± 5 [+1.58]. Additionally, $^1J(^{195}Pt-^{11}B)$ = 260 Hz for ^{11}B signal at δ −9.9. ^{31}P NMR (CDCl$_3$, 221 K) [ordered as: δ multiplicity, intensity, $^1J(^{195}Pt-^{31}P)$, $^2J(^{31}P-^{31}P)$/Hz)]: −16.3, s, 1P, 3299 ± 5, 36; −16.5, s, 1P, 3284 ± 5, 36. For ^{1}H data from PMe groups see ref. 2. A second compound ($R_f = 0.3$) was recrystallised from CH_2Cl_2–hexane (3:2) as orange crystals of [3,3-(PMe$_2$Ph)$_2$-*closo*-3,1,2-PtC$_2$B$_9$H$_{11}$] **3** (0.010 g, 4.4%) (Found: C, 35.9; H, 5.80. C$_{18}$H$_{33}$B$_9$P$_2$Pt requires C, 35.8; H, 5.50%). IR: ν_{max}(KBr) 2565s, 2530vs (sh), 2518vs, 2490s (sh) and 2460m (sh) cm^{-1} (BH). ^{11}B-{^{1}H} and ^{1}H-{^{11}B} NMR {CDCl$_3$, 294–298 K; ordered as δ(^{11}B), multiplicity, intensity, assignment [δ(^{1}H)]}: +5.7, s, 1B, B(8) [+3.66]; −9.2, s, 1B, B(10) [+4.15]; −9.9, s, 2B, B(9,12) [+2.28]; −14.5, s, 2B, B(5,11) [+1.91]; −20.8, s, 1B, B(6) [+2.05]; and −20.8, s, 2B, B(4,7) [+0.88]. Additionally, $^1J(^{195}Pt-^{11}B)$ 260 for B(8) and 170 for B(4,7), $^nJ(^{195}Pt-^1H)$ +39 (^2J) for B(8), −28 (^4J) for B(10), −38 (^3J) for B(9,12), <20 (^2J) for B(5,11) and +60 Hz (J) for B(4,7). δ(^{1}H) +2.98 for CH(1,2), for ^{1}H data from PMe groups see ref. 2. δ(^{195}Pt) −371 (Goodfellow scale).

Procedure (*b*), *reaction in solution at reflux for 6 d at atmospheric pressure*. This has been described in ref. 2. The two products isolated had identical TLC, R_f and spectroscopic properties to those of **5** (0.008 g, yield = 3.5%) and **3** (0.060 g, 26.4%).

Microwave irradiations of ethanolic solutions

[*nido*-7,8-$C_2B_9H_{12}$]$^-$. A mixture of Cs[7,8-$C_2B_9H_{12}$] (0.100 g, 0.376 mmol), ethanol (20 cm^3) and triethylamine (0.380 g, 3.76 mmol) was introduced into the microwave reaction vessel and subjected to microwave irradiation (650 W) for 30 min. The ethanol and triethylamine were removed under reduced pressure (rotary evaporator 35 °C). Spectroscopic (IR and ^{11}B NMR) data indicated that no rearrangement of the [7,8-$C_2B_9H_{12}$]$^-$ anion had occurred.

[3,3-$(PMe_2Ph)_2$-*closo*-3,1,2-$PtC_2B_9H_{11}$] 3. A solution of compound **3** (0.020 g, 0.033 mmol) in ethanol (20 cm^3) was introduced into the microwave reaction vessel and subjected to microwave irradiation (650 W) for 10 min. The ethanol was removed under reduced pressure (rotary evaporator, 35 °C). The reaction mixture was dissolved in CH_2Cl_2 and subjected to preparative TLC with CH_2Cl_2–hexane (3:2) as eluent. A single major product was recrystallised from CH_2Cl_2–hexane (3:2) as colourless crystals of **5** (0.018 g, 90.0%). Spectroscopic (IR and ^{11}B NMR) data and the R_f position were identical to those reported above.

Crystallography

Details of crystal data, data collection, structure solution and refinement for compounds **1** and **2** are summarised in Table 6. For **1** it was obvious from difference maps that the two As atoms in the arsenaborane cage were disordered unequally over the five sites adjacent to Pt; the atoms of that As_2B_3 ring were treated as 'As' atoms and their occupancies refined. The diagrams were drawn with the ORTEP program.[36]

Atomic coordinates, thermal parameters, and bond lengths and angles have been deposited at the Cambridge Crystallographic Data Centre (CCDC). See Instructions for Authors, *J. Chem. Soc., Dalton Trans.*, 1996, Issue 1. Any request to the CCDC for this material should quote the full literature citation and the reference number 186/131.

Acknowledgements

The generous loan of platinum salts by Johnson Matthey plc is gratefully acknowledged (T. R. S.). G. F. thanks the Natural Sciences and Engineering Research Council (Canada) for Research Grants, D. O'C. the Irish Science and Technology Funding Agency EOLAS (now FORBAIRT), J. D. K. the SERC (now EPSRC), UK for instrument support, and R. M. the Basque Government for a scholarship. We also thank Dr. B. Štíbr for his friendly interest and co-operation.

References

1 Part 12, J. P. Sheehan, T. R. Spalding, G. Ferguson, J. F. Gallagher, B. Kaitner and J. D. Kennedy, *J. Chem. Soc., Dalton Trans.*, 1993, 35.
2 D. O'Connell, T. R. Spalding, G. Ferguson, J. F. Gallagher and J. D. Kennedy, *J. Organomet. Chem.*, 1995, **501**, C12.
3 M. McGrath, T. R. Spalding, X. L. R. Fontaine, J. D. Kennedy and M. Thornton-Pett, *J. Chem. Soc., Dalton Trans.*, 1991, 3223.
4 Faridoon, O. Ni Dhubhghaill, T. R. Spalding, G. Ferguson, B. Kaitner, X. L. R. Fontaine and J. D. Kennedy, *J. Chem. Soc., Dalton Trans.*, 1989, 1657.
5 G. Ferguson, J. D. Kennedy, X. L. R. Fontaine, Faridoon and T. R. Spalding, *J. Chem. Soc., Dalton Trans.*, 1988, 2555.
6 D. M. P. Mingos, M. I. Forsyth and A. J. Welch, *J. Chem. Soc., Dalton Trans.*, 1978, 1363.
7 See, for example, E. A. Carroll, M. Green, F. G. A. Stone and A. J. Welch, *J. Chem. Soc., Dalton Trans.*, 1975, 2263; A. J. Welch, *J. Chem. Soc., Dalton Trans.*, 1975, 743; H. M. Colquhoun, T. J. Greenhough and M. G. H. Wallbridge, *J. Chem. Soc., Dalton Trans.*, 1979, 629.
8 D. R. Baghurst, R. C. B. Copley, H. Fleischer, D. M. P. Mingos, G. O. Kyd, L. J. Yellowlees, A. J. Welch, T. R. Spalding and D. O'Connell, *J. Organomet. Chem.*, 1993, **447**, C14.
9 K. A. Fallis, D. F. Mullica, E. L. Sappenfield and F. G. A. Stone, *Inorg. Chem.*, 1994, **33**, 4927; T. D. McGrath and A. J. Welch, *J. Chem. Soc., Dalton Trans.*, 1995, 1755.
10 R. Boese, A. Stanger, P. Stellberg and A. Shazar, *Angew. Chem., Int. Ed. Engl.*, 1993, **32**, 1475.
11 D. Braga, F. Grepioni, P. J. Dyson, B. F. G. Johnson, P. Frediani, M. Bianchi and F. Piacenti, *J. Chem. Soc., Dalton Trans.*, 1992, 2565.
12 J. A. Long, T. B. Marder, P. E. Behnken and M. F. Hawthorne, *J. Am. Chem. Soc.*, 1984, **106**, 2979; C. B. Knobler, T. B. Marder, E. A. Mizusawa, R. G. Teller, J. A. Long, P. E. Behnken and M. F. Hawthorne, *J. Am. Chem. Soc.*, 1984, **106**, 2990; J. A. Long, T. B. Marder and M. F. Hawthorne, *J. Am. Chem. Soc.*, 1984, **106**, 3004; *J. Chem. Soc., Chem. Commun.*, 1980, 677.
13 P. E. Behnken, J. A. Belmont, D. C. Busby, M. S. Delaney, R. E. King, C. W. Kreimendahl, T. B. Marder, J. J. Wilczynski and M. F. Hawthorne, *J. Am. Chem. Soc.*, 1984, **106**, 3011.
14 D. R. Baghurst and D. M. P. Mingos, *J. Chem. Soc., Dalton Trans.*, 1992, 1151.
15 S. A. Jasper, S. Roach, J. N. Stipp, J. C. Huffman and L. J. Todd, *Inorg. Chem.*, 1993, **32**, 3072.
16 J. D. Kennedy, B. Štíbr, M. Thornton-Pett and T. Jelínek, *Inorg. Chem.*, 1991, **30**, 4481; J. D. Kennedy, K. Nestor, B. Štíbr, M. Thornton-Pett and G. S. A. Zammitt, *J. Organomet. Chem.*, 1992, **447**, C1; J. D. Kennedy, B. Štíbr, T. Jelínek, X. L. R. Fontaine and M. Thornton-Pett, *Collect. Czech. Chem. Commun.*, 1993, **58**, 2090.
17 X. L. R. Fontaine, N. N. Greenwood, J. D. Kennedy, K. Nestor, M. Thornton-Pett, S. Hermanek, T. Jelínek and B. Štíbr, *J. Chem. Soc., Dalton Trans.*, 1990, 681.
18 M. Bown, J. Plešek, K. Base, B. Štíbr, X. L. R. Fontaine, N. N. Greenwood and J. D. Kennedy, *Magn. Reson. Chem.*, 1989, **27**, 947.
19 X. L. R. Fontaine, J. D. Kennedy, M. McGrath and T. R. Spalding, *Magn. Reson. Chem.*, 1991, **29**, 711.
20 G. Ferguson, J. F. Gallagher, M. McGrath, J. P. Sheehan, T. R. Spalding and J. D. Kennedy, *J. Chem. Soc., Dalton Trans.*, 1993, 27.
21 S. K. Boocock, N. N. Greenwood and J. D. Kennedy, *J. Chem. Soc., Chem. Commun.*, 1990, 305; S. K. Boocock, N. N. Greenwood, J. D. Kennedy, W. S. McDonald and J. Staves, *J. Chem. Soc., Dalton Trans.*, 1981, 2573.
22 B. Štíbr, T. Jelínek, J. D. Kennedy, X. L. R. Fontaine and M. Thornton-Pett, *J. Chem. Soc., Dalton Trans.*, 1993, 1261.
23 S. R. Bunkhall, X. L. R. Fontaine, N. N. Greenwood, J. D. Kennedy and M. Thornton-Pett, *J. Chem. Soc., Dalton Trans.*, 1990, 73.
24 S. A. Jasper, J. C. Huffman and L. J. Todd, *Inorg. Chem.*, 1995, **34**, 6430.
25 B. E. Mann, in *Comprehensive Organometallic Chemistry*, ed. G. Wilkinson, Pergamon, Oxford, 1982, vol. 3, p. 89.
26 N. L. Douek and A. J. Welch, *J. Chem. Soc., Dalton Trans.*, 1993, 1917.
27 G. Ferguson, M. C. Jennings, A. J. Lough, S. Coughlan, T. R. Spalding, J. D. Kennedy, X. L. R. Fontaine and B. Štíbr, *J. Chem. Soc., Chem. Commun.*, 1990, 891.
28 Y. L. Graft, Y. A. Ustynyuk, A. H. Borisenko and N. T. Kuznetsov, *Zh. Neorg. Khim.*, 1983, **28**, 2234.
29 M. Green, J. L. Spencer and F. G. A. Stone, *J. Chem. Soc., Dalton Trans.*, 1979, 6719.
30 G. B. Kauffman and D. O. Cowan, *Inorg. Synth.*, 1960, **6**, 211.
31 J. Plešek, S. Heřmánek and B. Štíbr, *Inorg. Synth.*, 1983, **22**, 231.
32 T. P. Hanusa, N. R. de Parisi, J. G. Kester, A. Arafat and L. J. Todd, *Inorg. Chem.*, 1987, **26**, 4100.
33 W. R. Pretzer and R. W. Rudolph, *J. Am. Chem. Soc.*, 1976, **98**, 1441.
34 R. J. Goodfellow, in *Multinuclear NMR*, ed. J. Mason, Plenum, London and New York, 1987.
35 W. McFarlane, *Proc. R. Soc. London, Ser. A*, 1968, **36**, 185.
36 C. K. Johnson, ORTEP II, Report ORNL-5138, Oak Ridge National Laboratory, Oak Ridge, TN, 1976.
37 A. C. Larsen, *Crystallographic Computing*, Munksgaard, Copenhagen, 1970, p. 203.
38 W. Clegg, *Acta Crystallogr., Sect. A*, 1987, **37**, 22.
39 E. J. Gabe, Y. LePage, J. P. Charland, F. J. Lee and P. S. White, *J. Appl. Crystallogr.*, 1989, **22**, 384.
40 G. M. Sheldrick, SHELXL 93, A program for the refinement of crystal structures, University of Göttingen, 1993.

Received 31*st January* 1996; *Paper* 6/00735J